Drying characteristics and quality attributes of quick-cooking Job's tears as affected by rotary drying combined with microwave heating

MATHA SINTHUKOT – SURACHET SUANJAN – PRARIN CHUPAWA – SUDATHIP INCHUEN – FREDERIK RONSSE – WASAN DUANGKHAMCHAN

Summary

A combined microwave heating and rotary drying process was developed to prepare the quick-cooking Job's tears. Using operating parameters of hot air temperature (70–90 °C), microwave power (150–450 W) and rotational drum speed (0.17–0.50 s^{-1}), drying characteristics were described using the Page drying model. The model parameters (drying rate constant k and power constant n) considerably correlated with drying factors using the quadratic equation. Drying time (DT) predicted by the Page model and effective diffusivity coefficient (D_e) ranged from 42 min to 116 min and from 487.69 × 10^{-8} $m^2 \cdot s^{-1}$ to 1 249.96 × 10^{-8} $m^2 \cdot s^{-1}$, respectively. The proposed drying technique resulted in lower DT and higher D_e, while utilizing less energy than hot air drying. Response surface methodology showed the influence of all operating factors on drying rate constant (k), DT, D_e, and specific energy consumption (SEC). Optimal drying conditions were determined by maximizing k and D_e while minimizing DT and SEC as air temperature of 76 °C with 450 W microwave heating and 0.17 s^{-1} rotational drum speed. Quality attributes of quick-cooking Job's tears prepared by drying under such optimal conditions were comparable to those prepared by conventional cooking and freeze-drying. Findings of this study can be used for practical application of Job's tears grains.

Keywords

adlay; rotary drying; drying model; microwave heating; quick-cooking grain; response surface

Job's tears grains (*Coix lachryma-jobi* L.) are a significant functional food in Asia, renowned for both culinary and nutraceutical uses [1] due to their health benefits [2, 3]. However, their high amylose content, which limits water absorption and swelling, leads to problematic lengthy soaking and cooking times [3–5]. This may hinder modern consumers seeking convenience.

Considering the growing preference for quick-cooking grains due to their convenient preparation, this study bears significant relevance. Starch-based products like instant rice, derived from drying pre-gelatinized or fully gelatinized grains, are a representative example in this context. Recognizing that the drying process crucially influences the quality attributes of instant foods [6–8], various drying techniques have been explored, including air drying [9–11], microwave drying [8], infrared radiation heating [12, 13], and freeze-drying [9–11, 14]. Among these, freeze-drying is a highly efficient method promising desirable rehydration properties and preservation of the organoleptic qualities of freshly cooked grains, though it is costly and time-consuming.

Matha Sinthukot, Surachet Suanjan, Department of Mechanical Engineering, Faculty of Engineering, Mahasarakham University, Kamriang, Kantarawichai, Maha Sarakham 44150, Thailand.
Prarin Chupawa, Research Unit of Mechatronics Engineering, Faculty of Engineering, Mahasarakham University, Kamriang, Kantarawichai, Maha Sarakham 44150, Thailand; Research Unit of Smart Process Design and Automation, Faculty of Engineering, Mahasarakham University, Kamriang, Kantarawichai, Maha Sarakham 44150, Thailand.
Sudathip Inchuen, Department of Food Technology, Faculty of Technology, Mahasarakham University, Kamriang, Kantarawichai, Maha Sarakham 44150, Thailand.
Frederik Ronsse, Department of Green Chemistry and Technology, Faculty of Bioscience Engineering, Ghent University, Coupure Links 653, B-9000 Ghent, Belgium.
Wasan Duangkhamchan, Research Unit of Smart Process Design and Automation, Faculty of Engineering, Mahasarakham University, Kamriang, Kantarawichai, Maha Sarakham 44150, Thailand; Research Unit of Process Design and Automation, Faculty of Engineering, Mahasarakham University, Kamriang, Kantarawichai, Maha Sarakham 44150, Thailand.

Correspondence author:
Wasan Duangkhamchan, e-mail: wasan.d@msu.ac.th

The research focusing on enhancing drying techniques for quick-cooking grains has seen substantial growth recently. Previous studies by CHEN et al. [4] and CHUPAWA et al. [8] investigated the expensive infrared-assisted freeze-drying method and an energy-efficient combined microwave fluidized bed technique for various grain types. Our study extended the boundaries of this existing research, introducing a novel method combining rotary drying with microwave heating, a cost-effective and energy-efficient process for producing quick-cooking Job's tears grain. Our hypothesis asserts that this innovative approach will enhance drying efficiency while preserving organoleptic qualities of quick-cooking Job's tears grains, thereby illustrating the scientific novelty of our research.

Consequently, this study introduced an innovative solution to the preparation complexities of quick-cooking Job's tears grains by suggesting a distinctive approach, a combination of rotary drying and microwave heating. We explored the drying characteristics of cooked Job's tears grains and examined a range of operational parameters. The aim was to identify optimal drying conditions, which would ultimately contribute to improving the overall efficiency of quick-cooking grain processing. This objective demonstrated our commitment to expanding knowledge in this field.

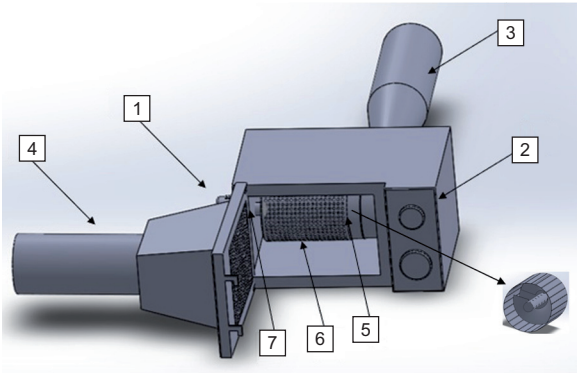

Fig. 1. Laboratory-scale device for rotary drying combined with microwave heating.

1 – direct current motor, 2 – microwave power controller, 3 – inlet air duct, 4 – outlet air duct, 5 – drilled spindle, 6 – rotary perforated drum, 7 – cavity cover.

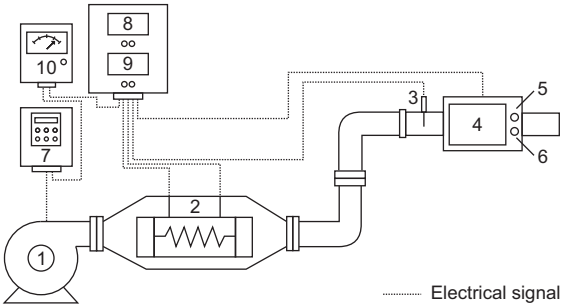

Fig. 2. Schematic diagram of the control system.

1 – air blower, 2 – heating box, 3 – thermocouple, 4 – microwave cavity, 5 – microwave power knob, 6 – timer, 7 – inverter, 8 – temperature controller, 9 – rotational speed controller, 10 – power supply unit.

MATERIALS AND METHODS

Materials and sample preparation

Job's tears grains (JTG) were purchased from a local supermarket in Maha Sarakham Province, Thailand. The sorted grains were soaked in warm distilled water with a grain-to-water ratio of 1 : 3 for 2 h in an insulated container. After soaking, 150 g of the grains were cooked in 450 ml of boiling water for 45 min. During the cooking process, the sample was checked by compressing one kernel between two glasses until the uncooked chalky core disappeared [15]. Finally, the completely cooked grains were packed in an aluminium foil bag and then subjected to the drying process. Samples prepared by soaking in excess water for 7 h and cooking for 45 min in boiling water were considered as traditionally cooked JTG, following ARLAI and KIETBUNSRI [5] with some modifications.

Equipment

A perforated drum with an internal conveying screw was positioned inside a domestic microwave oven MS23F300EEK (Samsung, Seoul, South Korea) to enable radial and axial sample movement, as depicted in Fig. 1. Power modulation in the oven utilized pulse width modulation. Fig. 2 illustrates the microwave power control, facilitated by a regulating knob (number 5), and a timer (number 6) set to specific durations. Ambient air, supplied by a blower (number 1), was heated in an electric box (number 2) before entering the microwave oven (number 4) through a spindle. A proportional–integral–derivative temperature controller (number 8) Model MAC-3D (Shimax, Akita, Japan), connected to a thermocouple (number 3), measured the air temperature at the chamber entrance and adjusted the heater power. This sufficiently long and narrow thermocouple, inserted into an air current, measured the air temperature. It was sheathed in a fine metallic close-ended tube and the junction of the thermocouple ensured thermal contact with the tube

tip, which was in thermal equilibrium with the air passing over it on the outside. A microcontroller (number 9) determined the drum rotational speed, allowing bidirectional motion and influencing grain activity within. The combined energy usage of the microwave oven, air blower and heating system was measured by an electricity meter (number 10).

Drying procedure

For each experimental run, 200 g of cooked samples were placed inside the drying drum. The three operating parameters tested were hot air temperature ranging from 70 °C to 90 °C, microwave power ranging from 150 W to 450 W and rotational speed ranging from 0.17 s^{-1} to 0.50 s^{-1}. A 33 full factorial design was used to study the effects of these parameters and to optimize the drying conditions. All experimental runs were conducted with three replications.

Analysis of drying kinetics

Various drying conditions were tested to study drying characteristics and the effects of rotary drying combined with microwave heating on quick-cooking JTG samples. All JTG kernels were weighed every 5 min using a precision balance (± 0.002 g) DNA503 (XingYun, Jiangsu, China) to determine changes in moisture content over time. The sampling procedure was conducted quickly to minimize the overall process interuption. Experimental runs were stopped when the moisture content reached a steady state or approximately 10 % on wet basis (wb). Thin-layer drying modelling was conducted using a simplified Eq. 1 to describe the drying behaviour, with moisture ratio (*MR*) expressed as a function of drying time (*t*, expressed in minutes). The measured *MR* was fitted to the semi-empirical models listed in Tab. 1.

$$MR = \frac{M_t}{M_0} \tag{1}$$

where *M* denotes moisture content on dry basis (db), and subscript 0 and *t* represent moisture content at initial and any time, respectively.

Among several semi-empirical drying models, as summarized by Ertekin and Firat [16], the Page drying equation was used to describe the drying characteristics of quick-cooking JTG due to its high suitability and versatility for biological materials [17, 18]. The Page drying model contained two parameters including drying rate constant (*k*) and power constant (*n*), as expressed in Eq. 2. Non-linear regression was used to determine the model parameters for all drying conditions tested in this work. The coefficient of determination (R^2) and root mean square error (*RMSE*) were used to evaluate the model accuracy [16].

$$MR = \exp(-kt^n) \tag{2}$$

The model constants (*C*) obtained from the Page drying equation were then correlated with hot air temperature (*T*), microwave power (*MW*) and rotational drum speed (*RDS*) using linear (Eq. 3), quadratic (Eq. 4), logarithmic (Eq. 5), power (Eq. 6) and Arrhenius (Eq. 7) relationships (Tab. 2). All equation coefficients were estimated using a Quasi-New iterative method.

Effective coefficient of moisture diffusivity analysis

The effective coefficient of moisture diffusivity (D_e) was estimated using a semi-theoretical equation following Fick's second law. For spherical materials with diameter *d*, Eq. 8 was converted into a natural logarithm, thereby allowing the establishment of a linear relationship between ln(*MR*) and drying time (*t*). The slope of this straight line was determined and considered to be the De value [16].

$$MR = \frac{8}{\pi^2}\exp\left(-\frac{\pi^2}{d^2}D_e t\right) \tag{8}$$

Specific energy consumption

Energy consumed by air heating and microwave heating system was measured in kilowatt hours. Specific moisture evaporation rate (*SMER*) was determined by comparing the rate at which moisture evaporated (W_{evap}) in kilograms per hour with the total energy expended (*E*), and expressed as Eq. 9:

$$SMER = \frac{W_{evap}}{1000 \times E} \tag{9}$$

The specific energy consumption (*SEC*), the ratio of total energy to evaporated moisture, was calculated using Eq. 10 and expressed in megajouls per kilogram using a conversion factor of 3.6.

$$SEC = \frac{3.6 \times E}{W_{evap}} \times 1000 \tag{10}$$

Analysis of quality attributes

Moisture content and water activity

The standard oven method (AOAC 930.15) [19] was used to measure the moisture content of JTG and a water activity meter Aqualab 4 (Meter, Pullmann, Washington, USA) was used to measure water activity (a_w).

Tab. 1. Page model constants, energy efficiency and responses.

Drying conditions			Page model parameters		*DT* [min]	D_e [$\times 10^{-8}$ m^2·s^{-1}]	Energy efficiency			
T [°C]	*MW* [W]	*RDS* [s^{-1}]	*k*	*n*			W_{evap} [g·h^{-1}]	*E* [kWh]	*SMER* [kg·kWh^{-1}h^{-1}]	*SEC* [MJ·kg^{-1}]
70	150	0.17	0.0276	0.9032	97	576.13	62.08	0.18	0.36	10.15
70	150	0.33	0.0210	0.9224	104	487.69	52.31	0.26	0.20	17.96
70	150	0.50	0.0134	1.0840	84	684.04	60.98	0.29	0.21	17.30
70	300	0.17	0.0324	0.9412	65	819.27	56.84	0.30	0.19	18.86
70	300	0.33	0.0120	1.0461	102	498.86	44.17	0.43	0.10	35.75
70	300	0.50	0.0120	1.1267	72	716.66	53.08	0.42	0.13	28.80
70	450	0.17	0.0451	0.9358	51	1 200.05	119.82	0.46	0.26	13.75
70	450	0.33	0.0287	1.0280	53	1 052.85	113.34	0.82	0.14	25.99
70	450	0.50	0.0076	1.1606	60	944.62	85.26	0.66	0.13	27.89
80	150	0.17	0.0163	1.1425	58	1 012.45	79.25	0.20	0.40	8.90
80	150	0.33	0.0045	1.3710	76	770.84	74.64	0.23	0.33	11.01
80	150	0.50	0.0126	1.1604	66	848.62	74.94	0.28	0.27	13.37
80	300	0.17	0.0169	1.1713	50	1 107.33	101.40	0.51	0.19	18.62
80	300	0.33	0.0220	1.0712	53	969.67	95.09	0.60	0.16	23.05
80	300	0.50	0.0080	1.3050	57	920.11	82.15	0.47	0.17	20.80
80	450	0.17	0.0470	0.9416	42	1 207.07	95.56	0.48	0.20	18.36
80	450	0.33	0.0377	0.9088	63	907.74	91.53	0.63	0.15	24.71
80	450	0.50	0.0156	1.2157	42	1 223.84	94.92	0.63	0.15	23.87
90	150	0.17	0.0143	1.1680	61	978.28	103.43	0.27	0.38	9.57
90	150	0.33	0.0271	0.9870	66	850.54	95.88	0.27	0.35	10.33
90	150	0.50	0.0117	1.1323	79	728.15	70.51	0.25	0.28	12.77
90	300	0.17	0.0236	1.0551	54	967.80	87.23	0.44	0.20	18.12
90	300	0.33	0.0394	0.9127	58	944.14	88.29	0.24	0.37	9.69
90	300	0.50	0.0183	1.1002	58	915.00	85.88	0.43	0.20	18.16
90	450	0.17	0.0232	1.1175	44	1 249.96	107.61	0.69	0.16	23.06
90	450	0.33	0.0399	0.9761	45	1 238.18	106.45	0.66	0.16	22.25
90	450	0.50	0.0175	1.1613	49	1 119.10	105.19	0.62	0.17	21.30
70	0	0.33	0.0027	1.3423	116	476.87	44.60	0.36	0.12	29.26
80	0	0.33	0.0080	1.1593	98	588.66	57.09	0.38	0.15	23.99
90	0	0.33	0.0076	1.1603	97	555.75	58.78	0.31	0.19	19.10

T – temperature, *MW* – microwave power, *RDS* – rotational drum speed, *k* – drying rate constant, *n* – power constant, *DT* – estimated drying time, D_e – effective diffusivity coefficient, W_{evap} – water evaporation rate, *E* – total energy consumption, *SMER* – specific moisture evaporation rate, *SEC* – specific energy consumption.

Tab. 2. Relationship types between model constants and drying parameters.

Model	Equation	Eq.
Linear	$C = a_0 + a_1(T) + a_2(MW) + a_3(RDS)$	(3)
Quadratic	$C = a_0 + a_1(T) + a_2(MW) + a_3(RDS) + a_4(T)(MW) + a_5(T)(RDS) + a_6(MW)(RDS) + a_7(T)^2 + + a_8(MW)^2 + a_9(RDS)^2$	(4)
Logarithmic	$C = a_0 + a_1 \ln(T) + a_2 \ln(MW) + a_3 \ln(RDS)$	(5)
Power	$C = a_0(T)^{a_1}(MW)^{a_2}(RDS)^{a_3}$	(6)
Arrhenius	$C = a_0(MW)^{a_1}(RDS)^{a_2} \exp\left(-\frac{a_3}{T}\right)$	(7)

C – model constant, *T* – temperature, *MW* – microwave power, *RDS* – rotational drum speed.

Colour change

Colour change (ΔE) of dried JTG against unprocessed grains was evaluated using the CIE $L^*a^*b^*$ colour system, where L^*, a^*, and b^* represent lightness, redness and yellowness, respectively. The parameters were measured using a Minolta Colorimeter (Konica Minolta, Tokyo, Japan). Change in redness (Δa^*) and yellowness (Δb^*) were used to evaluate total colour change, expressed as Eq. 11.

$$\Delta E = \sqrt{(\Delta a^*)^2 + (\Delta b^*)^2} \quad (11)$$

Rehydration properties

The rehydration ratio (RR) was evaluated by rehydrating 10 g of dried JTG in 100 ml of boiling water for 10 min and was expressed as the ratio between rehydrated sample weight (w_r) and initial sample weight (w_i) using Eq. 12. This procedure was conducted rapidly with care to minimize any potential interruption of rehydration.

$$RR = \frac{w_r}{w_i} \quad (12)$$

The rehydration rate constant (k_r) measures the rate at which water is absorbed during the rehydration process. To determine this rate, 15 g of dried JTG were placed in 1 l of boiling water. To record the weight change as a function of time, all sample kernels were removed using a strainer and placed on a cotton cloth to minimize water on their surface. After weighing, these samples were returned to continue the rehydration process. The weight of the sample was recorded every minute (w_t) until it reached equilibrium (w_e). The weight gain on rehydration (WGR) expressed as Eq. 13 was fitted to the semi-empirical first-order kinetic model (Eq. 14) and the k_r value was then estimated using a non-linear regression method.

$$WGR = \frac{w_e - w_t}{w_e} \times 100 \quad (13)$$

$$WGR = WGR_e - (WGR_e - 1)\exp(-k_r t) \quad (14)$$

The rehydration time (RT) value was measured according to Luithui and Meera [15] with some modifications. Briefly, dried JTG (10 g) were immersed in 1 l of boiling water. A single kernel was removed at time intervals of 5 min and later of 30 s, and pressed between two glass slides. The RT value was defined as the time at which the grain had no uncooked chalky core.

Textural properties

A texture analyser TA-XT2i (Stable Micro Systems, Godalming, United Kingdom) was used to determine the hardness and stickiness of rehydrated JTG following the method of Luithui and Meera [15]. Ten kernels of cooked or rehydrated JTG were placed on a platform and compressed to 80% strain using a 35 mm cylindrical plunger at a speed of 1 mm·s^{-1}. The hardness and stickiness values were obtained from the compressive force vs distance curve and expressed as maximum force and negative force area, respectively.

Response surface methodology and process optimization

Response surface methodology (RSM) associated with 33 full factorial design was used to investigate the effects of drying parameters consisting of T, MW and RDS on drying performance and energy consumption. RSM associated with a non-linear polynomial equation (Eq. 15) was then used to optimize the dependent parameter.

$$Y_i = a_0 + a_1X_1 + a_2X_2 + a_3X_3 + a_4X_1X_2 + \\ + a_4X_1X_2 + a_5X_1X_3 + a_6X_2X_3 + a_7X_1^2 + \\ + a_8X_2^2 + a_9X_3^2 \quad (15)$$

In Eq. 15, X_1, X_2, and X_3 were defined as the control factors of T, MW and RDS, respectively, while Y_1, Y_2, Y_3 and Y_4 were the responses of k, DT, D_e and SEC, respectively. The desirability functions for each response, $d_i(Y_i)$, for maximum and minimum value were defined and subsequently used maximizing the overall desirability (D) expressed in Eq. 16 [20],

$$D = (d_1 \cdot d_2 \cdot d_2 \cdot \cdots \cdot d_m)^{1/m} \quad (16)$$

where m is total number of responses. Studentized residuals standardized raw residuals for consistent variance, enhancing model prediction reliability against experimental data. This involved normalizing residuals by their standard deviation, improving data-model comparison and identifying irregularities.

RESULTS AND DISCUSSION

Drying characteristics

Model accuracy was demonstrated by R^2 and $RMSE$ values, which were 0.98–1.00 and 0.0047–0.0316, respectively. Tab. 1 lists the Page model parameters, including the drying rate constant (k) and power constant (n), estimated drying time (DT) and effective diffusivity coefficient (D_e) under various conditions.

The drying rate constant (k) is a key indicator of the drying rate. In Tab. 1, this constant fluctuated between 0.0027 and 0.0470. The maximum

Tab. 3. Statistical parameters for selecting the correlation of *k* and *n* constants.

Model	*k*		*n*	
	R^2	*RMSE*	R^2	*RMSE*
Linear	0.46	0.0085	0.21	0.1144
Quadratic	0.69	0.0065	0.59	0.0819
Logarithm	0.40	0.0089	0.19	0.1172
Power	0.43	0.0088	0.17	0.1172
Arrhenius	0.43	0.0088	0.17	0.1173

k – drying rate constant, *n* – power constant, R^2 – coefficient of determination, *RMSE* – root mean squared error.

value was observed with a combination of 80 °C hot air drying, 450 W microwave heating and 0.17 s^{-1} rotational speed. Utilizing rotary drying in combination with microwave heating led to enhanced drying rates of cooked JTG compared to only rotary hot air drying, attributed to the augmented volumetric heat from microwaves [18]. The drying rates were influenced by microwave power, as higher intensities resulted in better thermal energy transfer, promoting rapid moisture vaporization [21]. However, microwave drying presents challenges of uneven electromagnetic fields, leading to material hot spots [22]. To mitigate this, the study ensured constant movement of JTG samples within the rotating drum. In this study, cooked JTG samples were moved in both radial and axial directions by a rotating drum with a screw inside. Tab. 1 shows that the *k* value decreased as the rotational drum speed increased, even with the same hot air temperature and microwave power.

Tab. 3 indicates that the quadratic correlation best fitted the data concerning *k* and *n* constants, presenting the highest R^2 and lowest *RMSE* values. The formulated drying equation, incorporating these constants, was derived from drying temperature (*T*), microwave power (*MW*) and rotational drum speed (*RDS*) according to Eq. 2, where constants *k* and *n* are given by Eq. 17 and Eq. 18 (Tab. 4).

Fig. 3 show the drying behaviour of JTG samples under hot air of constant 70 °C. The study incorporated various microwave intensities, ranging from 150 W to 450 W, and rotational velocities between 0.17 s^{-1} and 0.50 s^{-1}. As expected for biological materials, JTG exhibited an exponential decrease trend in moisture over duration of drying, similar to many biological materials [6, 18, 23–25]. Initial moisture in the JTG samples was determined at 51.1 ± 3.8 % (wb). The target was 10 % (wb) content, corresponding to *MR* of 0.2. As depicted in Fig. 3B, the rotary drying combined with microwave heating method demonstrated quicker drying (periods of 45–95 min) than rotary hot air drying (110 min), as further demonstrated in Tab. 1. Enhanced microwave power facilitated a quicker moisture reduction in JTG samples due to its superior volumetric heating. However, microwave drying efficiency is tempered by its potential for hotspot development due to electromagnetic field inconsistency. Nonetheless, continuous movement of the material during heating mitigates this issue [22, 26–28]. Fig. 3 suggest that maintaining a lower rotational speed ensures optimal microwave energy absorption and consistent drying. At higher speeds, cooked JTG moved faster in radial and axial directions, which resulted in grain accumulation at the leftmost or rightmost side of the rotating chamber, thereby resulting in stagnation of some grains. Therefore, a rotational speed of 0.17 s^{-1} was considered an appropriate parameter as it provided continuous motion of sample grains.

Drying behaviour of cooked JTG using rotary drying combined with microwave heating at hot air temperatures of 80 °C and 90 °C followed the same manner as it was affected by microwave power and rotational speed (data not shown). As reported elsewhere, increasing hot air temperature led to higher drying rate and shorter drying time [16].

Combination of microwave heating with hot air rotary drying

Tab. 1 also presents the effects of all drying factors on water evaporation rate (W_{evap}), total

Tab. 4. Best fitted quadratic correlations of Page model parameters with all drying factors.

Constants	Equation	Eq.
Drying rate constant	$k = 0.2658 - 5.8 \times 10^{-3}(T) + 5 \times 10^{-6}(MW) - 1.47 \times 10^{-3}(RDS) + 4.9 \times 10^{-5}(T)(RDS) - 3 \times 10^{-6}(MW)(RDS) + 3 \times 10^{-5}(T)^2 - 5.6 \times 10^{-5}(RDS)^2$	(17)
Power constant	$n = -6.0026 + 0.1676(T) + 1.08 \times 10^{-3}(MW) + 1.01 \times 10^{-2}(RDS) - 2.2 \times 10^{-5}(T)(MW) - 5.78 \times 10^{-4}(T)(RDS) + 3 \times 10^{-5}(MW)(RDS) - 9.23 \times 10^{-4}(T)^2 + 8.51 \times 10^{-4}(RDS)^2$	(18)

T – temperature, *MW* – microwave power, *RDS* – rotational drum speed.

energy consumption (E) and specific moisture evaporation rate ($SMER$). As depicted, using only hot air in rotary drying yielded W_{evap} values ranging from 44.60 g·h^{-1} to 58.78 g·h^{-1}, while the combined drying process led to an increase with a span from 44.17 g·h^{-1} to pronounced 119.82 g·h^{-1}. The combination of microwave heating with hot air rotary drying offers a dual-action mechanism: direct excitation of internal water molecules by microwaves facilitates rapid evaporation, while the combined approach disrupts the moist air boundary around the grain, typically seen in conventional hot air drying. This synergistic effect, coupled with uniform heating and enhanced thermal gradients, ensures a more pronounced moisture removal, leading to the elevated evaporation rates observed [18, 21].

Tab. 1 reveals that energy expenditure for hot-air rotary drying ranged between 0.31 kWh and 0.38 kWh, while when combining microwave heating with rotary drying, the energy consumption expanded, ranging from 0.18 kWh to 0.82 kWh. Interestingly, for all drying temperature settings combined with a microwave intensity of 150 W, energy utilization was notably lower than when solely relying on the hot air technique. This observation can be rationalized by the synergistic balance achieved between the internal moisture migration to the material surface, driven by the microwave volumetric heating, and the surface moisture transfer to the surrounding environment, facilitated by the convective heat mechanism.

Additionally, Tab. 1 demonstrates that both W_{evap} and E values fluctuated according to the specific drying method employed. To evaluate the effectiveness and efficiency of the drying processes, specific moisture evaporation rate ($SMER$) was computed based on the W_{evap} and E values. The data from Tab. 1 revealed that $SMER$ values in scenarios using only hot air for drying typically exhibited lower ranges, specifically between 0.12 kg·kWh^{-1}h^{-1} and 0.19 kg·kWh^{-1}h^{-1}. On the contrary, the $SMER$ readings for the combined drying approach were generally elevated, with a range from 0.10 kg·kWh^{-1}h^{-1} to 0.40 kg·kWh^{-1}h^{-1}, averaging at approximately 0.22 kg·kWh^{-1}h^{-1}. Consequently, it was evident that the synergistic utilization of hot-air rotary drying combined with microwave heating enhanced both drying efficiency and effectiveness.

Response surface methodology

Tab. 5 illustrates the drying factor impact and its quadratic relationship to all outcomes. The model, having an F-value of 4.12 and a mere 0.6 % noise probability, shows the significance of micro-

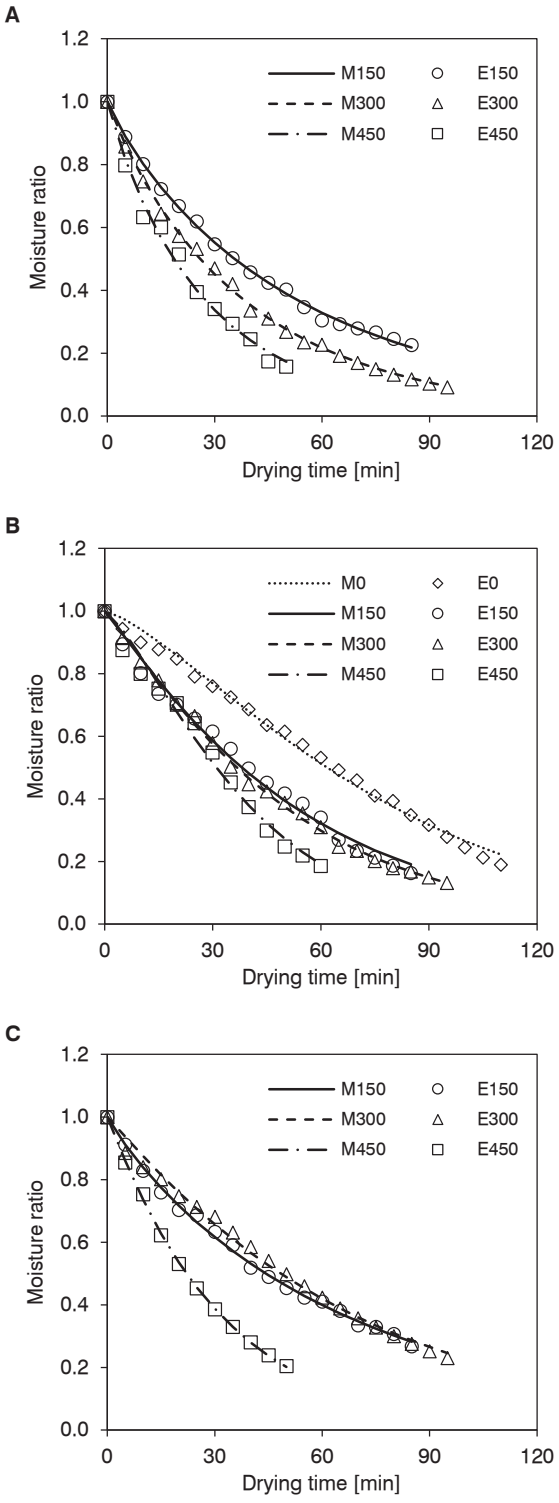

Fig. 3. Moisture ratio as a function of drying time at hot air temperature of 70 °C combined with variation of microwave power and rotational drum speed.

A – rotational drum speed 0.17 s^{-1}, B – rotational drum speed 0.33 s^{-1}, C – rotational drum speed 0.50 s^{-1}.
M0, M150, M300, M450 – model values at microwave power 0 W, 150 W, 300 W and 450 W, respectively. E0, E150, E300, E450 – experimental values at microwave power 0 W, 150 W, 300 W and 450 W, respectively.

wave power and rotational speed, evident from a *p*-value below 0.05. A discrepancy between the predicted R^2 (0.1989) and the adjusted R^2 (0.5195) raised questions about the model fit or potential overfitting issues. With a precision of 7.369, surpassing the desired 4, the model reliability was affirmed. Rotational speed primarily affected the drying rate constant, followed by microwave power and air temperature.

Model predictions were compared with experimental data through residual analyses, utilizing ANOVA and regression. Normal probability plots, essential for evaluating residual normality, aim to align with a normal distribution [20]. Fig. 4 shows these using studentized residuals. While most data points followed a pattern consistent with the model expectations, anomalies appeared, especially for *SEC* (Fig. 4D). Consequently, the model adequately aligned with the variance expectations shown in Fig. 4.

Fig. 5 illustrates 3D plots of *T* and *MW* effects on the drying rate constant (*k*) at rotational speeds of 0.17 s^{-1}, 0.33 s^{-1} and 0.50 s^{-1}. The graphs showed that increased air temperature and microwave

Tab. 5. Results of the fitted model analysis of variance (ANOVA) for responses.

Source	Approximate coefficient			
	k	*DT*	D_e	*SEC*
Model (*p* value)	0.0058 [b]	< 0.0001 [d]	< 0.0001 [d]	0.0008 [d]
Intercept				
a_0	0.022	61.85	880.11	22.12
Linear terms				
a_1X_1	0.0008 [ns]	–9.67 [d]	111.72 [d]	–2.85 [b]
a_2X_2	0.0063 [c]	–13.44 [d]	178.15 [d]	4.99 [d]
a_3X_3	–0.0072 [c]	2.50 [ns]	–56.57 [a]	2.49 [a]
Interaction terms				
$a_{12}X_1X_2$	0.0007 [ns]	4.42 [ns]	–33.28 [ns]	0.98 [ns]
$a_{13}X_1X_3$	0.0049 [ns]	2.00 [ns]	–15.30 [ns]	–0.69 [ns]
$a_{23}X_2X_3$	–0.0045 [ns]	0.083 [ns]	–5.29 [ns]	0.072 [ns]
Quadratic terms				
$a_{11}X_1^2$	0.003 [ns]	10.44 [a]	–109.11 [a]	0.90 [ns]
$a_{22}X_2^2$	0.0024 [ns]	0.11 [ns]	75.69 [ns]	–3.95 [a]
$a_{33}X_3^2$	–0.0056 [ns]	–8.39 [a]	98.75 [a]	–2.10 [ns]
***F* value**				
Model	4.12	8.65	9.88	5.92
X_1	0.19	20.45	19.32	8.47
X_2	10.76	39.55	49.12	26.08
X_3	13.98	1.37	4.95	6.52
X_1X_2	0.082	2.85	1.14	0.66
X_1X_3	4.29	0.58	0.24	4.28
X_2X_3	3.66	0.001	0.029	0.048
X_1^2	0.80	7.96	6.14	0.29
X_2^2	0.48	0.0009	2.96	5.43
X_3^2	2.86	5.13	5.03	1.53
Coefficient of determination R^2	0.6858	0.8208	0.8395	0.7582
Adjusted R^2	0.5195	0.7260	0.7546	0.6302
Predicted R^2	0.1989	0.5668	0.5980	0.4196
Adequate precision	7.369	11.302	11.748	8.38
Coefficient of variation [%]	37.07	14.33	11.68	22.19
Standard deviation	0.008	9.07	107.84	1.15

Lowercase letters in superscript indicate statistical significance (a – $p < 0.05$, b – $p < 0.01$, c – $p < 0.005$, D – $p < 0.001$, ns – not significant).
X_1 – temperature, X_2 – microwave power, X_3 – rotational drum speed, *k* – drying rate constant, *n* – power constant, *DT* – estimated drying time, D_e – effective diffusivity coefficient, *SEC* – specific energy consumption.

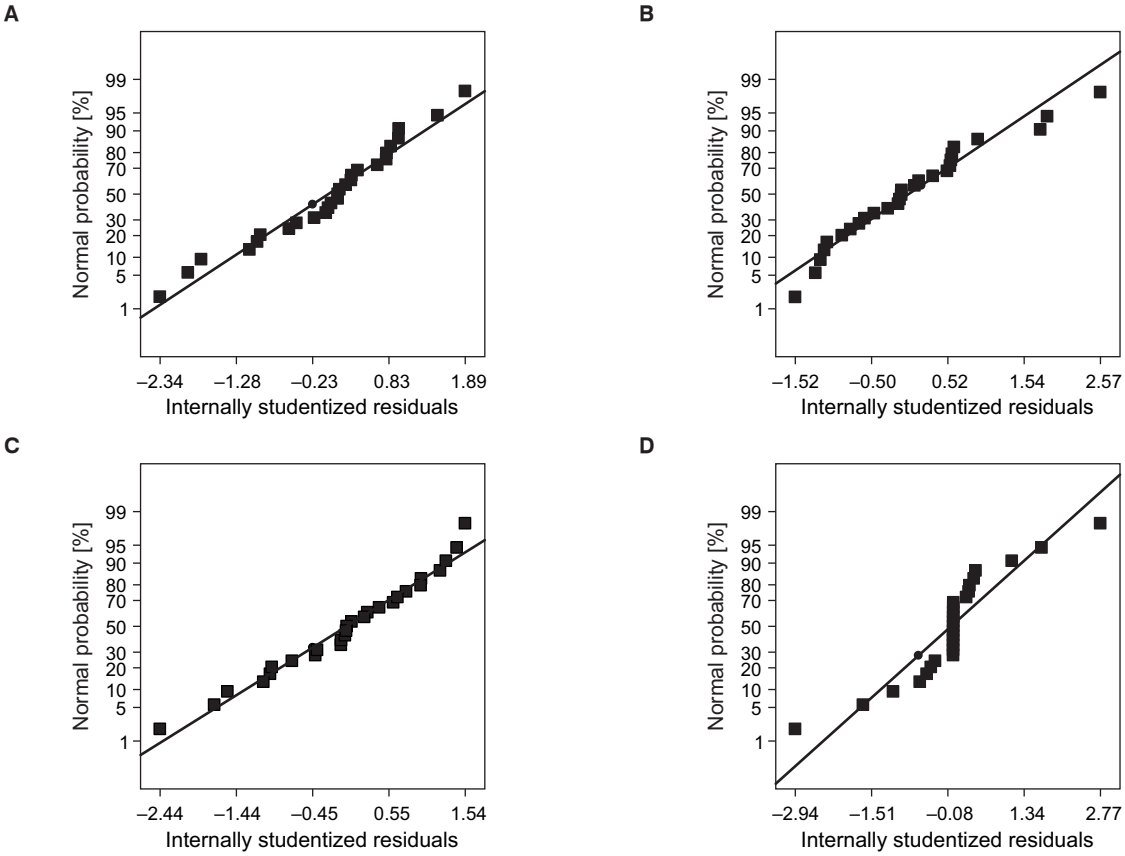

Fig. 4. Normal plot of residuals.

A – drying rate constant, B – drying time, C – effective diffusity, D – specific energy consumption.

power raised the *k* constant. Notably, at 0.17 s^{-1}, this effect was significant. In Fig. 5A, the *k* constant reached approximately 0.044 at 70 °C and 450 W, but dropped to 0.013 at 90 °C and 150 W. In Fig. 5B, at 0.33 s^{-1}, the peak *k* value was 0.036 at 90 °C and 450 W, whereas the lowest was 0.02 at 80 °C and 150 W, highlighting a linear microwave power impact on *k* and a quadratic air temperature effect. In Fig. 5C, at 0.50 s^{-1}, microwave adjustments brought about marginal shifts, but air temperature led to pronounced variations in *k*, with the peak (0.023) at 90 °C and 450 W and the lowest value (0.006) at 70 °C and 300 W.

Fig. 5C displays the lowest *k* value at peak rotational speed and 70 °C drying temperature, slightly affected by microwave power. Contrastingly, Fig. 5A and Fig. 5B exhibit a positive trend with temperature at rotational speeds of 0.17 s^{-1} and 0.33 s^{-1}. This variation might have been the result of the horizontal movement of cooked JTG, influenced by the drum internal conveyor rotation. Occasional misalignments in rotation caused material clustering at the drum ends, possibly impairing solid-air heat transfer and electromagnetic absorption, leading to uneven moisture evaporation.

Tab. 5 highlights the notable significance of the estimated drying time (*DT*) with an *F*-value of 8.65. The model robustness was further evidenced by the probability value ($Prob > F$), which was notably less than 0.0001, indicating a confidence level exceeding 95 % in the model predictive accuracy. Monomial values for *T* and *MW* were significant ($p < 0.001$), while *RDS* and all interaction terms were insignificant ($p > 0.05$). Among quadratic parameters, T^2 and RDS^2 were significant, contrasting with MW^2. With closely matching predicted R^2 (0.5668) and adjusted R^2 (0.7260) values, and the adequate precision of 11.302, the model effectively directed towards the targeted design. Moreover, Tab. 5 underscores microwave power as the dominant factor affecting *DT*, followed by air temperature and rotational speed.

Fig. 6 present 3D plots illustrating drying time (*DT*) at various rotational speeds. The plots highlight that increased *T* and *MW* corresponded to a higher *k* value, reducing drying time for a 10 % (wb) final moisture content. At 0.17 s^{-1} speed and 450 W microwave power, drying time

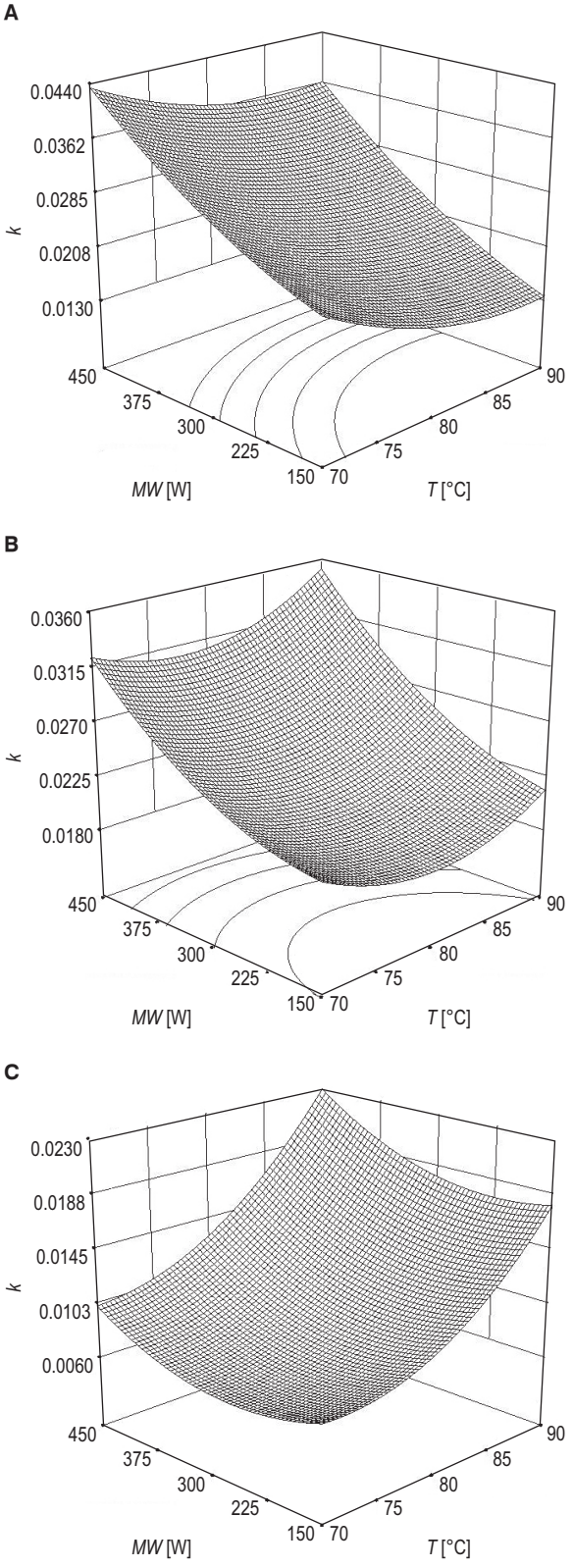

Fig. 5. Contour plots of drying rate constant.

A – rotational drum speed 0.17 s^{-1}, B – rotational drum speed 0.33 s^{-1}, C – rotational drum speed 0.50 s^{-1}.
k – drying rate constant, *MW* – microwave power, *T* – temperature.

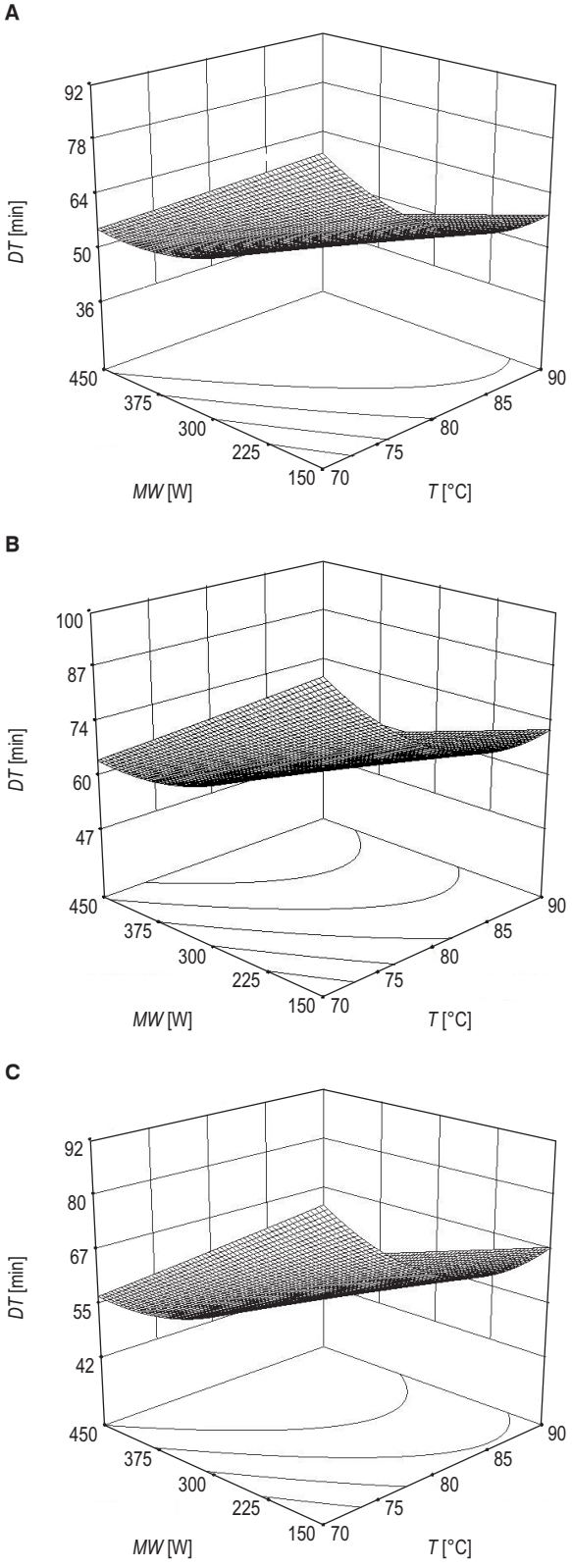

Fig. 6. Contour plots of drying time.

A – rotational drum speed 0.17 s^{-1}, B – rotational drum speed 0.33 s^{-1}, C – rotational drum speed 0.50 s^{-1}.
DT – estimated drying time, *MW* – microwave power, *T* – temperature.

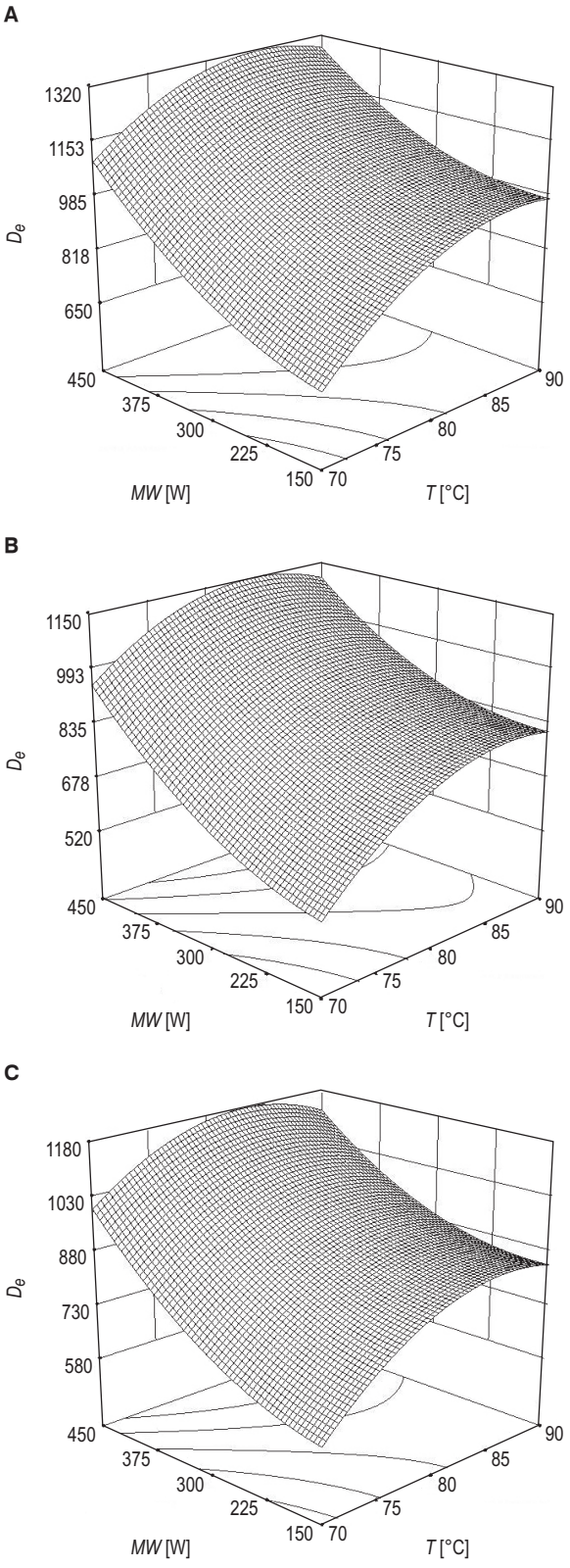

Fig. 7. Contour plots of effective diffusivity.

A – rotational drum speed 0.17 s^{-1}, B – rotational drum speed 0.33 s^{-1}, C – rotational drum speed 0.50 s^{-1}.
D_e – effective diffusivity coefficient, *MW* – microwave power, *T* – temperature.

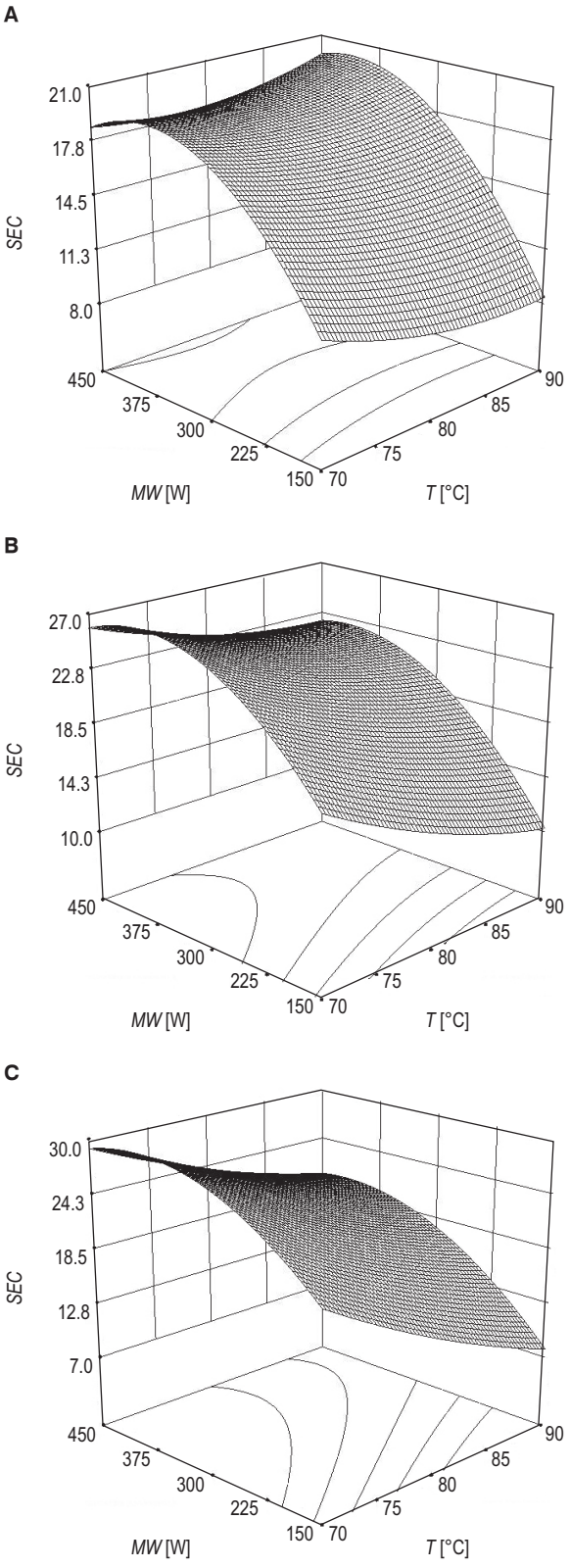

Fig. 8. Contour plots of the specific energy consumption.

A – rotational drum speed 0.17 s^{-1}, B – rotational drum speed 0.33 s^{-1}, C – rotational drum speed 0.50 s^{-1}.
SEC – specific energy consumption, *MW* – microwave power, *T* – temperature.

was approximately 37 min (Fig. 6C). Conversely, a prolonged drying time of 100 min was observed at 70 °C, 150 W microwave power and 0.33 s^{-1} speed (Fig. 6B). This trend persisted at high speeds, where shortest and longest durations were at 85 °C with 450 W and 70 °C with 150 W, respectively. Optimal drying matched the maximum drying rate constant at 0.17 s^{-1}.

Tab. 5 highlights the significance of the quadratic model for the effective diffusivity coefficient (D_e) with a p-value < 0.0001 and an F-value of 9.88. Monomial terms T and MW were significant at $p < 0.001$, while RDS was significant at $p < 0.05$. Interaction terms ($T \times MW$, $T \times RDS$, $MW \times RDS$) and MW^2 were insignificant ($p > 0.05$), yet T^2 and RDS^2 emerged as significant at $p < 0.05$. A predicted R^2 of 0.5980 aligned well with the adjusted R^2 of 0.7546. The adequate precision value of 11.748 surpassed the desired threshold of 4, affirming the model suitability for design space exploration. From Tab. 5, microwave power with an F-value of 49.12 was dominant, hot air temperature followed at 19.32, while rotational drum speed at 4.95 was less influential.

The D_e value indicates the speed of internal moisture diffusion to a material surface during the falling-rate drying period, with higher values suggesting quicker drying [21]. Fig. 7 shows 3D contour plots of D_e values in relation to hot air temperature and microwave power across various rotational speeds. These plots signify that both temperature and microwave power positively impacted D_e values, albeit with diverse linear and quadratic patterns. At 0.17 s^{-1} (Fig. 7A), the highest D_e value (1 320 × 10^{-8} $m^2 \cdot s^{-1}$) was attained at 85 °C with 450 W microwave power, while the lowest D_e value (650 × 10^{-8} $m^2 \cdot s^{-1}$) was at the minimal settings. As rotational speed decreased, D_e values were from 520 × 10^{-8} $m^2 \cdot s^{-1}$ to 1 150 × 10^{-8} $m^2 \cdot s^{-1}$ and from 580 × 10^{-8} $m^2 \cdot s^{-1}$ to 1 180 × 10^{-8} $m^2 \cdot s^{-1}$ at 0.33 s^{-1} and 0.50 s^{-1}, respectively.

Drying efficacy was evaluated via specific energy consumption (SEC), drying rate constant and effective diffusivity coefficient. Tab. 5 displays a significant second-order polynomial model for SEC with an F-value of 5.92 and a p-value of 0.0008. Monomial factors T, MW and RDS had p-values below 0.01, 0.001 and 0.05, respectively. Model terms $T \times MW$, $T \times RDS$, $MW \times RDS$, T^2 and RDS^2 were non-significant ($p > 0.05$), but MW^2 was significant ($p < 0.05$). R^2 values (predicted R^2 0.4196, adjusted R^2 0.6302) were consistent. With a precision of 8.38, the model showed robustness and MW was the primary factor due to its paramount F-value.

SEC quantifies the energy needed for moisture evaporation. Fig. 8 displays the impact of drying temperature and microwave power across varying rotational speeds. The optimum SEC was achieved at maximal temperature and minimal microwave intensity. Notably, at reduced rotation (Fig. 8A), microwave power had a greater influence on SEC than had temperature. Elevated microwave intensity expedited drying, hence reducing drying duration, but also led to a rise in SEC. Higher rotational speeds typically resulted in increased SEC.

The data presented in Tab. 5 and the various contour and diagnostic plots indicated that the quadratic polynomial model was a suitable tool for navigating design space and optimization. However, removing any insignificant terms also enhanced model accuracy.

Multiple response optimization

Previous studies revealed that the drying rate constant (k), estimated drying time (DT), effective diffusivity coefficient (D_e) and specific energy consumption (SEC) were influenced by hot air temperature, microwave power and rotational speed in different ways. The best combination of these variables was explored to optimize the process. The goal of this study was to determine the optimal values for all variables by maximizing k and D_e, while minimizing DT and SEC using a desirability function.

Results in Tab. 6 showed that the best desirability area ranged from 0.837 to 0.850. The combination of hot air temperature 76 °C, microwave power 450 W and rotational speed 0.17 s^{-1} resulted in the highest desirability of 0.85, making it the globally optimal method for rotary drying combined with microwave heating to produce quick-cooking JTG.

Quality attributes

Tab. 7 compares the quality attributes of JTG dehydrated and rehydrated using our proposed drying technique under optimal conditions with those obtained from other methods.

Moisture content of quick-cooking JTG dried by rotary drying combined with microwave heating was 10.4 ± 0.1 % (wb), similar to the moisture content of raw JTG (10.2 ± 0.1 %). The moisture content of the sample after freeze-drying was extremely low (0.2 ± 0.0 %) because of the moisture sublimation stage in the drying process [9, 10, 14]. This low moisture content resulted in low a_w of 0.0230 ± 0.0002. The proposed drying method resulted in a slightly higher a_w (0.3046 ± 0.0033) compared to the raw sample (0.2428 ± 0.0011) but still fell within safe levels (< 0.6) for storing biological materials.

Tab. 6. Optimal drying conditions based on highest desirability.

Factors			Responses				Desirability
T [°C]	*MW* [W]	*RDS* [s^{-1}]	*k* [min^{-1}]	*DT* [min]	D_e [$\times 10^{-8}$ $m^2 \cdot s^{-1}$]	*SEC* [$MJ \cdot kg^{-1}$]	
76.59	450.00	0.17	0.0385	41.23	1249.95	5.05	0.850
76.50	450.00	0.17	0.0385	41.36	1248.42	5.05	0.850
76.40	449.99	0.17	0.0386	41.51	1246.63	5.05	0.850
76.77	448.75	0.17	0.0383	41.10	1249.97	5.06	0.849
75.78	450.00	0.17	0.0389	42.46	1235.60	5.05	0.848
76.91	447.74	0.17	0.0381	41.01	1249.96	5.07	0.847
77.81	450.00	0.17	0.0379	39.64	1268.74	5.06	0.846
76.39	445.23	0.17	0.0381	42.00	1235.53	5.08	0.843
76.96	450.00	0.18	0.0381	42.00	1238.48	5.20	0.839
80.89	450.00	0.17	0.0367	36.99	1302.01	5.10	0.837

T – temperature, *MW* – microwave power, *RDS* – rotational drum speed, *k* – drying rate constant, *DT* – estimated drying time, D_e – effective diffusivity coefficient, *SEC* – specific energy consumption.

Tab. 7. Quality attributes of dried and rehydrated samples obtained using various methods.

Attribute	Drying methods			
	Raw sample	Traditionally cooked	Freeze-dried	Proposed method
MC [%]	10.2 ± 0.1^{a}	–	0.2 ± 0.0^{b}	10.4 ± 0.1^{a}
a_w	0.2428 ± 0.0011^{b}	–	0.0230 ± 0.0002^{c}	0.3046 ± 0.0033^{a}
Colour				
*L** (lightness)	69.17 ± 0.25^{b}	–	73.55 ± 0.18^{a}	61.17 ± 0.06^{c}
*a** (redness)	2.49 ± 0.04^{a}	–	1.32 ± 0.02^{c}	2.23 ± 0.02^{b}
*b** (yellowness)	19.50 ± 0.16^{b}	–	14.89 ± 0.03^{c}	19.96 ± 0.03^{a}
ΔE (colour change)	–	–	6.46 ± 0.12^{b}	8.02 ± 0.05^{a}
Rehydration properties				
Rehydration ratio		–	1.32 ± 0.02^{a}	0.897 ± 0.01^{b}
Rehydration rate constant		–	0.3086 ± 0.0081^{a}	0.1002 ± 0.0106^{b}
Rehydration time [min]		–	10 ± 1^{b}	20 ± 3^{a}
Textural properties				
Hardness [g]	–	$18\,628.12 \pm 1461.63^{a}$	$7\,916.37 \pm 1\,220.15^{b}$	$16\,573.02 \pm 2\,216.45^{a}$
Stickiness [g·s]	–	-185.75 ± 7.93^{b}	-67.43 ± 22.75^{a}	-82.53 ± 20.41^{a}

Superscripts represent significant difference of the means in the same row ($p \leq 0.05$).
MC – moisture content (expressed on wet basis), a_w – water activity.

Maintaining the colour quality of processed products is crucial for ensuring consumer acceptance. The L^*, a^* and b^* values of samples dried using various methods such as freeze-drying and rotary drying combined with microwave heating were measured. The resulting colour change (ΔE) was then calculated. The proposed drying method resulted in darker L^* value (61.17 ± 0.06) compared to the raw material but redness a^* (2.23 ± 0.02) and yellowness b^* (19.96 ± 0.03) values were comparable to the raw sample. The freeze-dried sample was the lightest but had the lowest values of redness and yellowness. Our proposed drying method resulted in a slight colour change of 8.02 ± 0.05, which was comparable to ΔE obtained by freeze drying (6.46 ± 0.12). Therefore, our proposed method met the required criterion for colour quality.

Instant or quick-cooking products require good rehydration properties. In this study, the rehydration ratio, rate constant and rehydration time of the samples prepared by the proposed drying method were compared to those prepared by freeze-drying. Results in Tab. 7 show that rotary drying in combination with microwave heating gave a lower rehydration ratio and rate constant with longer rehydration time. This suggested that JTG dried using the proposed method had lower water absorption capacity during rehydration compared to those prepared by freeze-drying, which

usually creates a porous structure that allows for faster water absorption [9–11, 14].

The textural properties of rehydrated JTG prepared using rotary drying combined with microwave heating, freeze-drying and traditional cooking methods were also determined. Results in Tab. 7 show that our proposed method produced a sample with hardness similar to the traditionally cooked sample but significantly higher hardness than the freeze-dried sample. The softer texture of the freeze-dried sample was due to more water absorption during rehydration [29]. Insignificant difference in stickiness between samples produced using both drying methods was observed, but significantly lower than that prepared by traditional cooking. Based on these findings, rotary drying combined with microwave heating is considerably a good option for producing quick-cooking JTG with desirable textural properties.

CONCLUSIONS

This study explored the efficacy of rotary drying combined with microwave heating for producing quick-cooking Job's tears grains. Experimentation with variations of drying temperature, microwave power and rotational drum speed demonstrated the effectiveness of Page equation in describing the drying characteristics. With a pronounced impact of microwave power on all responses, optimal conditions were 76 °C inlet temperature, 450 W microwave power and 0.17 s^{-1} drum speed, based on optimization of efficiency parameters. Crucially, these results, consistent with our hypothesis, revealed that this processing method not only enhanced drying efficiency but also maintained the organoleptic characteristics of the quick-cooking Job's tears grains in line with traditional and freeze-drying benchmarks, underscoring the scientific and practical merit of our proposed method.

Acknowledgements

This research project was financially supported by Mahasarakham University.

REFERENCES

1. Li, J. – Corke, H.: Physicochemical properties of normal and waxy job's tears (*Coix lachryma-jobi* L.) starch. Cereal Chemistry, *76*, 1999, pp. 413–416. DOI: 10.1094/cchem.1999.76.3.413.
2. Yu, F. – Gao, J. – Zeng, Y. – Liu, C. X.: Effects of adlay seed oil on blood lipids and antioxidant capacity in hyperlipidemic rats. Journal of the Science of Food and Agriculture, *91*, 2011, pp. 1843–1848. DOI: 10.1002/jsfa.4393.
3. Bunthawong, O. – Jomduang, S.: The optimal drying temperature and moisture content for microwavable job's tears grains. Chiang Mai University Journal of Natural Sciences, *15*, 2016, pp. 163–173. ISSN: 1685-1994.
4. Chen, K. – Zhang, M. – Bhandari, B. – Chen, J.: Instant quinoa prepared by different cooking methods and infrared-assisted freeze drying: Effects of variables on the physicochemical properties. Food Chemistry, *370*, 2022, article 131091. DOI: 10.1016/j.foodchem.2021.131091.
5. Arlai, A. – Kietbunsri, S.: Effects of soaking, steaming and vacuum microwave heating on structure and physical property of quick cooking Job's tear. Journal of Thai Interdisciplinary Research, *12*, 2017, pp. 16–21. DOI: 10.14456/jtir.2017.3.
6. Gaewsondee, T. – Duangkhamchan, W.: A novel process for preparing instant riceberry using fluidized bed drying assisted with swirling compressed air: Kinetic aspects. Food and Bioprocess Technology, *12*, 2019, pp. 1422–1434. DOI: 10.1007/s11947-019-02306-x.
7. Chupawa, P. – Gaewsondee, T. – Duangkhamchan, W.: Drying characteristics and quality attributes affected by a fluidized-bed drying assisted with swirling compressed-air for preparing instant red jasmine rice. Processes, *9*, 2021, article 1738. DOI: 10.3390/pr9101738.
8. Chupawa, P. – Inchuen, S. – Jaisut, D. – Ronsse, F. – Duangkhamchan, W.: Effects of stepwise microwave heating and expanded bed height control on the performance of combined fluidized bed/microwave drying for preparing instant brown rice. Food and Bioprocess Technology, *16*, 2023, pp. 199–215. DOI: 10.1007/s11947-022-02933-x.
9. Akintayo, O. A. – Adegbaju, K. E. – Akeem, S. A. – Balogun, M. A. – Adediran, O. J. – Aruna, T. E. – Onwudinjo, H. O. – Akintayo, F. M. – Adesina, B. O. – Ojo, P. K. – Kolawole, F. L. K.: Effect of parboiling and drying pretreatment on the cooking time and quality attributes of bambara groundnut. Journal of Food Processing and Preservation, *45*, 2021, article e15351. DOI: 10.1111/jfpp.15351.
10. Aravindakshan, S. – Nguyen, T. H. A. – Kyomugasho, C. – Buvé, C. – Dewettinck, K. – van Loey, A. – Hendrickx, M. E.: The impact of drying and rehydration on the structural properties and quality attributes of pre-cooked dried beans. Foods, *10*, 2021, article 1665. DOI: 10.3390/foods10071665.
11. Aravindakshan, S. – Nguyen, T. H. A. – Kyomugasho, C. – Van Loey, A. – Hendrickx, M. E.: The rehydration attributes and quality characteristics of 'Quick-cooking' dehydrated beans: Implications of glass transition on storage stability. Food Research International, *157*, 2022, article 111377. DOI: 10.1016/j.foodres.2022.111377.
12. Nachaisin, M. – Jamradloedluk, J. – Niamnuy, C.: Application of combined far-infrared radiation and air convection for drying of instant germinated

brown rice. Journal of Food Process Engineering, *39*, 2016, pp. 306–318. DOI: 10.1111/jfpe.12226.
13. Lang, G. H. – Timm, N. da S. – Neutzling, H. P. – Ramos, A. H. – Ferreira, C. D. – de Oliveira, M.: Infrared radiation heating: A novel technique for developing quick-cooking rice. LWT, *154*, 2022, article 112758. DOI: 10.1016/j.lwt.2021.112758.
14. Fu, T. – Niu, L. – Wu, L. – Xiao, J.: The improved rehydration property, flavor characteristics and nutritional quality of freeze-dried instant rice supplemented with tea powder products. LWT, *141*, 2021, article 110932. DOI: 10.1016/j.lwt.2021.110932.
15. Luithui, Y. – Meera, M. S.: Effect of heat processing on the physicochemical properties of Job's tears grain. Journal of Food Measurement and Characterization, *13*, 2019, pp. 874–882. DOI: 10.1007/s11694-018-0001-4.
16. Ertekin, C. – Firat, M. Z.: A comprehensive review of thin-layer drying models used in agricultural products. Critical Reviews in Food Science and Nutrition, *57*, 2017, pp. 701–717. DOI: 10.1080/10408398.2014.910493.
17. Tylewicz, U. – Mannozzi, C. – Castagnini, J. M. – Genovese, J. – Romani, S. – Rocculi, P. – Rosa, M. D.: Application of PEF- and OD-assisted drying for kiwifruit waste valorisation. Innovative Food Science and Emerging Technologies, *77*, 2022, article 102952. DOI: 10.1016/j.ifset.2022.102952.
18. Lazarin, R. A. – Zanin, R. C. – Silva, M. B. R. – Ida, E. I. – Berteli, M. N. – Kurozawa, L. E.: Drying kinetic and bioactive compounds of okara dried in microwave-assisted rotating-pulsed fluidized bed dryer. Food and Bioprocess Technology, *16*, 2023, pp. 565–575. DOI: 10.1007/s11947-022-02955-5.
19. Horwitz, W. (Ed.): Official methods of analysis of AOAC International. 17th edition. Gaithersburg : AOAC International, 2002. ISBN: 0935584676.
20. Majdi, H. – Esfahani, J. A. – Mohebbi, M.: Optimization of convective drying by response surface methodology. Computers and Electronics in Agriculture, *156*, 2019, pp. 574–584. DOI: 10.1016/j.compag.2018.12.021.
21. Zielinska, M. – Michalska, A.: Microwave-assisted drying of blueberry (*Vaccinium corymbosum* L.) fruits: Drying kinetics, polyphenols, anthocyanins, antioxidant capacity, colour and texture. Food Chemistry, *212*, 2016, pp. 671–680. DOI: 10.1016/j.foodchem.2016.06.003.
22. Monteiro, R. L. – Gomide, A. I. – Link, J. V. – Carciofi, B. A. M. – Laurindo, J. B.: Microwave vacuum drying of foods with temperature control by power modulation. Innovative Food Science and Emerging Technologies, *65*, 2020, article 102473. DOI: 10.1016/j.ifset.2020.102473.
23. Bórquez, R. – Melo, D. – Saavedra, C.: Microwave–vacuum drying of strawberries with automatic temperature control. Food and Bioprocess Technology, *8*, 2015, pp. 266–276. DOI: 10.1007/s11947-014-1400-0.
24. Chong, C. H. – Figiel, A. – Law, C. L. – Wojdyło, A.: Combined drying of apple cubes by using of heat pump, vacuum-microwave, and intermittent techniques. Food and Bioprocess Technology, *7*, 2014, pp. 975–989. DOI: 10.1007/s11947-013-1123-7.
25. Raut, S. – Md Saleh, R. – Kirchhofer, P. – Kulig, B. – Hensel, O. – Sturm, B.: Investigating the effect of different drying strategies on the quality parameters of *Daucus carota* L. using dynamic process control and measurement techniques Food and Bioprocess Technology, *14*, 2021, pp. 1067–1088. DOI: 10.1007/s11947-021-02609-y.
26. Nanvakenari, S. – Movagharnejad, K. – Latifi, A.: Multi-objective optimization of hybrid microwave-fluidized bed drying conditions of rice using response surface methodology. Journal of Stored Product Research, *97*, 2022, article 101956. DOI: 10.1016/j.jspr.2022.101956.
27. Taheri, S. – Brodie, G. – Gupta, D.: Microwave fluidised bed drying of red lentil seeds: Drying kinetics and reduction of botrytis grey mold pathogen. Food and Bioproducts Processing, *119*, 2020, pp. 390–401. DOI: 10.1016/j.fbp.2019.11.001.
28. Babaki, A. – Askari, G. – Emam-Djomeh, Z.: Drying behavior, diffusion modeling, and energy consumption optimization of *Cuminum cyminum* L. undergoing microwave-assisted fluidized bed drying. Drying Technology, *38*, 2020, pp. 224–234. DOI: 10.1080/07373937.2019.1652638.
29. Bui, L. T. T. – Coad, R. A. – Stanley, R. A.: Properties of rehydrated freeze-dried rice as a function of processing treatments. LWT, *91*, 2018, pp. 143–150. DOI: 10.1016/j.lwt.2018.01.039.

Received 27 June 2023; 1st revised 21 July 2023; 2nd revised 3 August 2023; 3rd revised 19 September 2023; accepted 2 October 2023; published online 2 February 2024.